Proc. Natl. Acad. Sci. USA
Vol. 88, pp. 8651–8655, October 1991
Medical Sciences

Acidic fibroblast growth factor promotes vascular repair

(vascular injury/angioplasty/tissue repair/endothelial cells/smooth muscle cells)

THORIR D. BJORNSSON*, MACIEJ DRYJSKI*, JOHN TLUCZEK*, ROBERT MENNIE†, JOHN RONAN†, THEODORE N. MELLIN†, AND KENNETH A. THOMAS†‡

*Division of Clinical Pharmacology, Department of Medicine, Jefferson Medical College, Thomas Jefferson University, Philadelphia, PA 19107; and †Department of Biochemistry, Merck Sharp & Dohme Research Laboratories, Rahway, NJ 07065

Communicated by P. Roy Vagelos, July 12, 1991

ABSTRACT **Intravascular injury to arteries can result in thickening of the intimal smooth muscle layer adjacent to the lumen by migration and proliferation of cells from the underlying medial smooth muscle layer accompanied by deposition of extracellular matrix. This pathological response, which decreases lumen diameter, might, in part, be the result of the access of smooth muscle cells to plasma and platelet-derived growth factors as a consequence of denudation of the overlying confluent monolayer of vascular endothelial cells. Injured rat carotid arteries were treated by i.v. administration of acidic fibroblast growth factor, a heparin-binding protein that is chemotactic and mitogenic for vascular endothelial cells. The growth factor treatment resulted in dose-dependent inhibition of intimal thickening with parallel promotion of endothelial regeneration over the injured area. Therefore, acidic fibroblast growth factor might be efficacious in the prevention of restenosis caused by intimal thickening following angioplasty in humans.**

Arterial architecture consists of an inner nonthrombogenic monolayer of vascular endothelial cells residing on a basement membrane covering thin intimal and thicker underlying medial layers of smooth muscle. Response to extensive arterial endothelial injury is characterized by migration and proliferation of medial smooth muscle cells into the intima, perhaps mediated by plasma- and platelet-derived growth factors, with the accumulation of extracellular matrix resulting in thickening of the intimal layer thereby decreasing vascular lumen diameter (1–3).

In animal models of limited arterial injury, spontaneous endothelial regeneration results in the cessation of both smooth muscle cell proliferation and intimal thickening (4–6). However, since vascular endothelium appears to have a limited ability to spontaneously repopulate denuded areas, repair of larger intravascular injuries can be incomplete (7). Therefore, specific mitogenic and chemotactic stimulation of vascular endothelial cells might promote arterial repair.

Several vascular endothelial cell mitogens have been identified, including platelet-derived endothelial cell growth factor (8), vascular endothelial cell growth factor (9–11), and many (12, 13), but not all (14), members of the fibroblast growth factor (FGF) family. The heparin-binding FGF family is composed of seven known homologous members. Acidic FGF (aFGF), one of the more extensively characterized family members, is both mitogenic (15) and chemotactic (16) for vascular endothelial cells *in vitro* and promotes blood vessel growth, or angiogenesis, *in vivo* (15, 17, 18). We describe the results of a series of experiments demonstrating that aFGF also both promotes repair of experimentally damaged rat arterial endothelium and inhibits the accompanying pathological intimal thickening.

The publication costs of this article were defrayed in part by page charge payment. This article must therefore be hereby marked "*advertisement*" in accordance with 18 U.S.C. §1734 solely to indicate this fact.

MATERIALS AND METHODS

Intravascular Injury. Endothelial injuries were produced in the right common carotid arteries of anesthetized male Sprague–Dawley rats (Charles River Breeding Laboratories) weighing 382 ± 72 g (mean ± SD). An ≈1-cm-long segment of each vessel was ligated at both ends. Blood was rinsed out with sterile saline and the endothelium was desiccated by using compressed air as described (4, 19). Ligatures were removed and gentle local pressure was applied until hemostasis was achieved.

aFGF Treatment. Pure human recombinant aFGF (20) was serially diluted in 0.9% NaCl/0.1% bovine serum albumin/standard clinical grade heparin (8.5 μg/ml; ≈1.3 units/ml) (heparin sodium USP; Scientific Protein Laboratories, Waunakee, WI) to final concentrations of 2, 20, 200, 670, 2.0×10^3, and 2.0×10^4 ng/ml. Each animal received aFGF at one of these concentrations either as a constant-rate i.v. infusion for 2 weeks or as a single i.v. bolus injection immediately after completion of surgery. The 2-week i.v. infusions were delivered from subcutaneously implanted miniosmotic pumps (0.2-ml reservoir; Alzet model 2002; Alza), which delivered aFGF through polyethylene catheters into the left jugular veins. Adjusted for body weight, the i.v. infusion rates of aFGF and animal group sizes, n, were 2.9 (n = 3), 26 (n = 5), 130 (n = 8), 270 (n = 9), and 870 (n = 5) $pg \cdot kg^{-1} \cdot hr^{-1}$ and 2.6 (n = 9) and 27 (n = 6) $ng \cdot kg^{-1} \cdot hr^{-1}$. Bolus 1-ml injections of aFGF were administered via the penile vein at doses of 0.060 (n = 4), 0.46 (n = 3), and 4.8 (n = 7) μg/kg. The amounts of heparin delivered as an aFGF stabilizer (20, 21) for constant rate and bolus dosing were 0.0015 $unit \cdot kg^{-1} \cdot hr^{-1}$ and 4.0 units/kg, respectively. Control groups received either no infusion (n = 9) or a heparin-containing vehicle placebo (n = 5).

Measurement of Intimal Thickening. Two weeks after injury, a time at which the intimal thickening response is well developed and characterized (4), carotid arteries were recovered for histological analysis. One hour before sacrifice, anesthetized animals were administered an i.v. injection of Evan's blue dye (60 mg/kg) (Fisher), fixed *in situ* for 10 min by retrograde perfusion of either 3.5% glutaraldehyde in 50 mM Pipes buffer (pH 7.4) or 10% formaldehyde/0.06% zinc sulfate, and excised (4). Evan's blue dye leaks into the vessel walls in regions of damaged endothelium and serves as a marker of injury (22).

The effect of aFGF dose level on intimal thickening response was determined from glutaraldehyde-fixed 5-μm-thick cross-sections through the vascular injuries. Histological sections were stained by a modified Verhoeff–van Gieson and Masson trichrome technique, photographed in color at

Abbreviations: FGF, fibroblast growth factor; aFGF, acidic FGF; I/M, intima/media cross-sectional area ratio; BS-I, *Bandeiraea simplicifolia* I lectin.

‡To whom reprint requests should be addressed at: Merck Sharp & Dohme Research Laboratories, Room 80W-243, P.O. Box 2000, Rahway, NJ 07065.

×4 magnification, and the medial and intimal areas were quantitated by using a MacTablet model MM1201 digitizer (Summagraphics, Fairfield, CT). The location of maximal intimal thickness within each vessel was determined by examining multiple histological sections spanning the central region of the vascular injury. The mean medial cross-sectional areas in mm^2 of the individual aFGF-treated dose groups, which ranged from 0.087 to 0.108, were not significantly different (two-tailed unpaired Student's *t* test) from either the vehicle control group (0.099 ± 0.012; mean ± SD) or the overall average of all vessels (0.098 ± 0.022). Since medial cross-sectional area reflects vessel size but does not change in response to aFGF treatment, intimal thickening was expressed as the ratio of intima/media (I/M) cross-sectional areas (23) to compensate for differences in vessel sizes among animals. The statistical significances of dose–response relationships were computed by fitting the percentage inhibition of I/M versus the logarithms of aFGF dose by linear regression analysis (19, 24).

Specific Staining of Vascular Endothelial Cells. A more extensive analysis was performed on a subset of formaldehyde-fixed vessels in conjunction with the analysis of endothelial coverage in which the entire length of each vascular injury was spanned within a set of cross-sections cut at 500-μm intervals (13–20 sections per vessel). These I/M area ratios and percentage coverage of the vessel inner perimeters by endothelial cells, visualized after staining with *Bandeiraea simplicifolia* I lectin (BS-I lectin; also called *Griffonia simplicifolia* I or GS-I), were quantitated on each section using a Joyce–Loebl full color Magiscan MD image analyzer system (Compix, Mars, PA).

The BS-I lectin technique for visualizing rat endothelial cells (25) was modified to amplify staining signal. BS-I lectin (30 μg of isolectin B_4 per ml; this and other immunoreagents were from Vector Laboratories) was added to hydrogen peroxide- and serum-blocked sections followed by overnight incubation with affinity-purified goat anti-BS-I primary antibody (1.0 μg/ml). Affinity-purified biotinylated rabbit anti-goat secondary antibody (7.5 μg/ml) was added followed 1 hr later by avidin linked to horseradish peroxidase (Vectastain ABC peroxidase kit). After 40 min, lectin–antibody complexes were visualized by deposition of peroxidase-oxidized diaminobenzidine. Sections were counterstained with Masson trichrome without Weigert's hematoxylin to prevent masking of the oxidized diaminobenzidine chromagen stain. Negative controls in which the BS-I lectin was omitted resulted in no detectable deposition of stain. Vascular endothelium was quantitated as the percentage of the inner perimeter of each vessel covered by BS-I-labeled endothelial cells visualized after image enhancement to improve stain to background contrast.

RESULTS

Intimal Thickening Response to Vascular Damage. Normal rat carotid arteries have virtually no detectable intimal smooth muscle layer (I/M = 0). Compared to uninjured controls (Fig. 1*A*), both untreated and vehicle control-treated (Fig. 1*B*) animals developed marked intimal thickening of the carotid arteries. Morphometric analysis of the arteries in untreated animals 2 weeks after injury revealed an average I/M ratio of 0.97. The thickened intima is primarily composed of smooth muscle cells and extracellular matrix (4, 19).

Inhibition of Intimal Thickening by aFGF. Animals treated with optimal doses of aFGF administered i.v. by either continuous infusion or bolus injection exhibited a substantial decrease in intimal thickening (Fig. 1*C*). In contrast, aFGF caused no detectable change in the thickness of the surrounding medial smooth muscle layer. Neither the intima nor media of the contralateral artery thickened in response to any of the infusion or bolus aFGF doses.

With increasing i.v. infusion rates of aFGF, the observed inhibition of intimal thickening increased to a maximum of 80% at 870 $pg \cdot kg^{-1} \cdot hr^{-1}$ (Fig. 2*A*). The correlation between aFGF infusion rate and inhibition of intimal thickening is statistically significant in this dose range ($P < 0.001$; total $n = 35$). At higher infusion rates of 2.6 and 27 $ng \cdot kg^{-1} \cdot hr^{-1}$

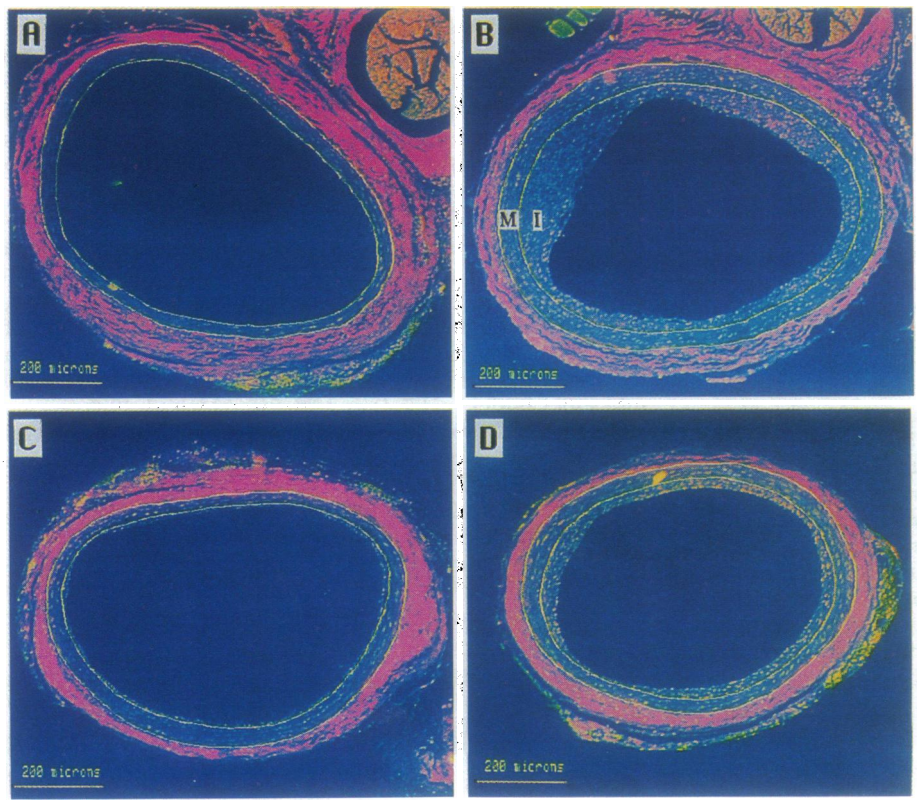

FIG. 1. Histological cross-sections of rat carotid arteries. Masson trichrome-stained and image-enhanced cross-sections are shown that are representative of normal uninjured rat carotid arteries (*A*) and of arteries 2 weeks after air-desiccation injury treated with either the vehicle control (*B*), optimal dose aFGF (*C*), or higher suboptimal dose of aFGF (*D*). Cross-sectional area ratios of the intima (I) divided by the media (M), artificially bordered by yellow lines, were 0.00 (*A*), 0.97 (*B*), 0.25 (*C*), and 0.60 (*D*). I/M ratios of aFGF-treated vessels (*C* and *D*) correspond to 75% and 38% inhibition, respectively. (Bars = 200 μm.)

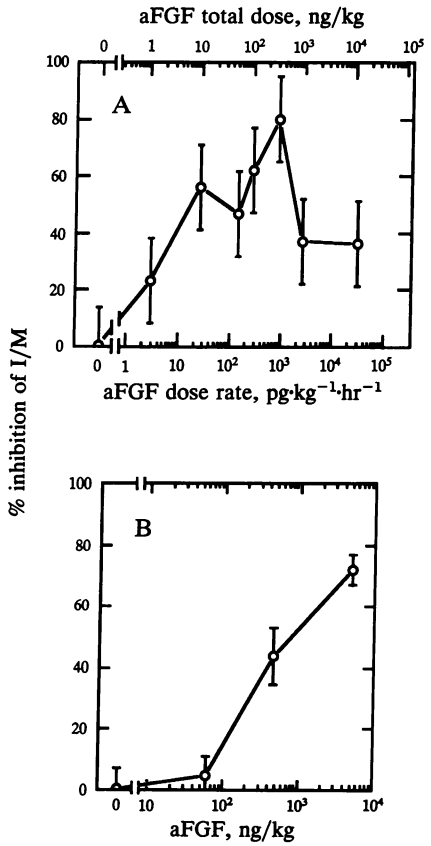

FIG. 2. Effect of aFGF dose on intimal thickening response. Percentage inhibition of the intimal thickening 2 weeks after injury, calculated as I/M ratio of central sections to normalize for vessel diameters, is shown as a function of aFGF dose. Effects of 2-week constant rate i.v. infusions (*A*) and single i.v. bolus injections of aFGF immediately after injury (*B*) were determined. Vertical error bars represent SEMs.

aFGF still inhibited intimal thickening albeit by 35–40% (Fig. 1*D*). The mechanism of the decreased inhibition of the I/M ratios at these higher dose levels is not attributable to an increase in medial cross-sectional areas, which, expressed as means ± SD in mm^2, are 0.098 ± 0.025 and 0.100 ± 0.020, respectively, versus 0.099 ± 0.012 for the vehicle control group.

Single i.v. injections of aFGF elicited a similar dose-dependent inhibition of intimal thickening, reaching 73% in response to a dose of 4.8 μg/kg (Fig. 2*B*). Although the response was qualitatively equivalent to that observed with continuous i.v. infusion, a single i.v. dose of nearly 20-fold more aFGF was required to achieve a quantitatively similar extent of inhibition. The relation between increasing single doses and greater inhibition of intimal thickening was also statistically significant ($P < 0.001$; total $n = 19$).

Endothelial Repair and Intimal Thickening. Both the I/M ratio and percentage endothelial coverage were determined in each cross-section obtained at 500-μm intervals throughout the entire injured regions of five aFGF-treated and six vehicle control-treated vessels. The aFGF-treated animals received the mitogen at 1.1 ng·kg^{-1}·hr^{-1}, an infusion rate intermediate between the optimally efficacious and higher suboptimal doses (Fig. 2*A*). Composite profiles of I/M ratio as a function of section level were generated by averaging equivalent section levels after alignment of the individual profiles to achieve the maximum cross-correlation between one vessel and all others in each treatment group. The same procedure was used to optimally align the average aFGF- and vehicle control-treated group profiles with each other.

The profiles of I/M ratio versus section level (Fig. 3 *Upper*) demonstrate that aFGF, even at a dose resulting in suboptimal efficacy, decreases not only maximal intimal thickening but also its longitudinal span. Examples of sections approximating the maximum I/M ratios of these averaged vehicle control-treated and aFGF-treated vessel profiles are shown in Fig. 1 *B* and *D*. Since the medial cross-sectional area does not change in response to either injury or treatment, the average volume of intima is proportional to the area under the I/M profile. Treatment with aFGF decreases the average intimal volume by one-half.

Endothelial cells were identified on the luminal surface of the vascular cross-sections by BS-I lectin staining as exemplified in Fig. 4 before and after image enhancement. The endothelial monolayer typically appears intact over areas of no intimal thickening, whereas it is either discontinuous or absent over regions of intimal thickening. Some BS-I-positive endothelial cells either are embedded in the intimal layer or remain attached to the buried basement membrane.

The average fraction of the inner vascular perimeter denuded of BS-I-staining endothelial cells, generated as a function of section level using the relative alignment offsets calculated for the I/M ratios, is presented in Fig. 3 (*Lower*). The areas above the aFGF-treated and vehicle control-treated curves reflect average total endothelial cell denudation. Both the width and the total denuded surface area of the aFGF-treated group are approximately one-half of the vehicle control-treated group. For the vehicle control and aFGF treatment groups, the average I/M ratio and fractional endothelial cell denudation curves (Fig. 3) are nearly mirror images of one another. The correlation coefficient between the I/M ratio and fractional endothelial denudation for the averaged section levels (Fig. 5) is 0.93 for all sections, 0.90 for vehicle control-treated, and 0.98 for aFGF-treated vessels.

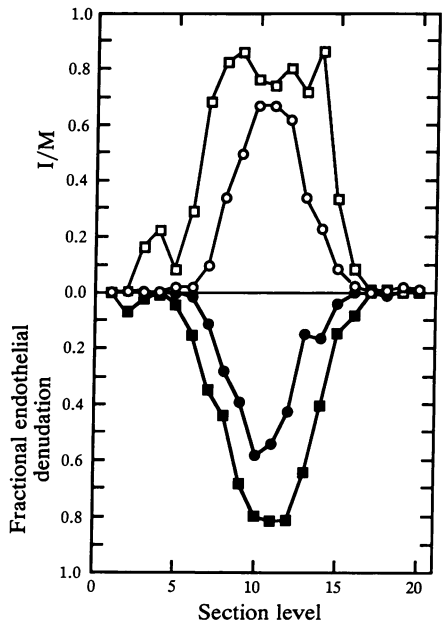

FIG. 3. Morphometric analysis spanning the length of injured arteries. Five aFGF-treated (circles) and six vehicle control-treated (squares) vessels were sectioned at 500-μm intervals through the length of the injuries. I/M cross-sectional area ratios as a function of section level, shown as open symbols (*Upper*), were averaged after alignment to achieve the maximum correlation coefficient between a common vessel and all others within each group. The same relative alignments were used to determine the averaged fractional endothelial denudation, measured as fraction of luminal perimeter devoid of endothelial cells. These average fractional denudation values are plotted as a function of section level with solid symbols (*Lower*).

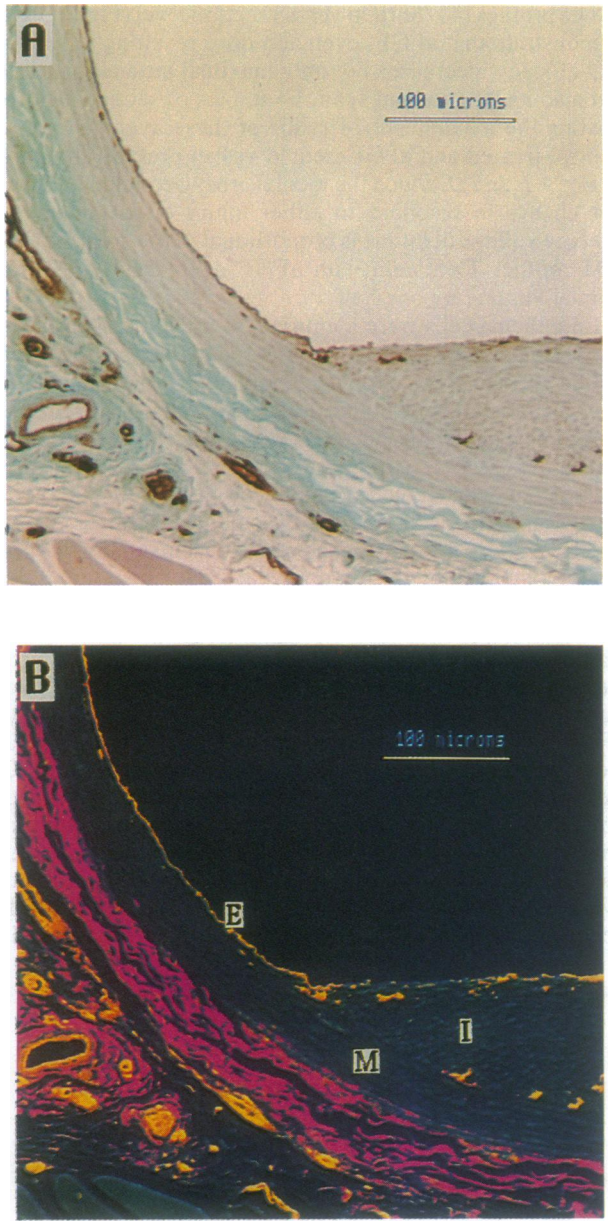

FIG. 4. BS-I lectin/immunoperoxidase staining of endothelial cells. A BS-I lectin-stained cross-section of an injured rat carotid artery is shown both before (*A*) and after (*B*) image enhancement. Specific lectin binding to rat endothelial cells was amplified by a double antibody technique visualized by deposition of brown peroxidase-oxidized stain and Masson trichrome counterstaining. The image was computationally enhanced to improve contrast by shifting the brown specific stain to yellow and the light tan medial and intimal staining to blue. Endothelial cells (E), media (M), and intima (I) are labeled in *B*. (Bars = 100 μm.)

DISCUSSION

aFGF is known to be a potent mitogenic and chemotactic substance for large vessel and microvascular endothelial cells in tissue culture and to promote angiogenesis *in vivo*. These data clearly demonstrate that aFGF also promotes repair of damaged vascular endothelium *in vivo*. In addition, aFGF in these dose ranges elicits a concomitant inhibition of pathological intimal thickening in rat carotid arteries responding to controlled intravascular injuries.

Remarkably low doses of aFGF are required both to promote repair of the vascular endothelial cell monolayer and to inhibit intimal thickening. The efficacy of aFGF at these

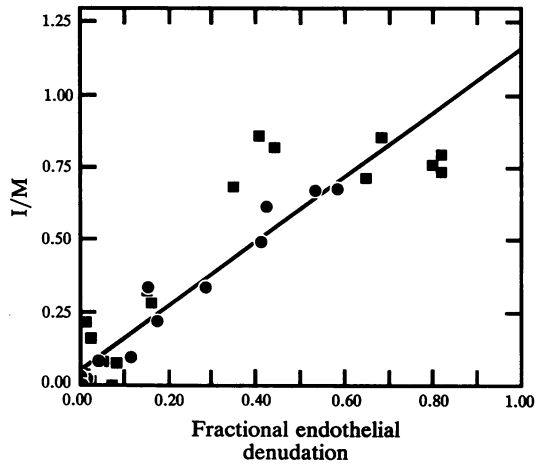

FIG. 5. Correlation between thickened intima and absence of endothelium. I/M cross-sectional ratios are plotted as a function of fractional endothelial denudation for each averaged section of aFGF-treated (circles) and vehicle control-treated (squares) vessels used to generate the composite response plot shown in Fig. 4. Overall, vehicle control, and aFGF-treated correlation coefficients are 0.93, 0.90, and 0.98, respectively.

low doses might, in part, reflect partitioning of this circulating heparin-binding growth factor onto the exposed heparan sulfate-containing subendothelial basement membrane and extracellular matrix, effectively concentrating the protein at sites of injury (26, 27). The requirement for a greater single dose of aFGF to elicit efficacy equivalent to that achieved with a nearly 20-fold lower total dose of continuously infused aFGF could be attributable to the rapid clearance of the circulating mitogen. Single bolus i.v. injections (3 and 60 μg/kg) of ^{125}I-labeled aFGF are cleared from plasma with an initial half-life of 3–4 min followed by a slower terminal half-life of 4–7 hr (28). Therefore, the maintenance of aFGF above an effective threshold for the minimum duration required to achieve efficacy would be expected to require a greater initial dose.

The mechanism of the aFGF-induced inhibition of intimal proliferation at sites of intravascular injury is unknown. Efficacy is not the result of the small amounts of heparin added to stabilize the protein. Although large doses of heparin alone can inhibit intimal thickening in this model, perhaps by mobilizing endogenous heparan proteoglycan-bound FGFs (29), untreated and vehicle control-treated vessels responded identically. This result would be expected since the heparin dose used in the present study is only ≈3% the minimal amount required to inhibit intimal thickening (19).

Parallel stimulation of endothelial repair, as evaluated by specific BS-I lectin/immunoperoxidase staining, accompanies inhibition of intimal thickening in response to continuous i.v. infusion of aFGF. The most straightforward mechanistic hypothesis to account for the efficacious inhibition of intimal thickening involves direct mitogenic and chemokinetic stimulation of vascular endothelial cells by circulating aFGF. Furthermore, exogenous aFGF that binds to subendothelial cell basement membrane heparan proteoglycans exposed at the site of intravascular injury could support not only mitogenesis but also two-dimensional chemotaxis or haptotaxis. Repair of damaged endothelium might, for example, inhibit intimal thickening by limiting exposure of the underlying smooth muscle cells to plasma- and platelet-derived growth factors and chemotactic substances such as insulin-like growth factor I and platelet-derived growth factor. Alternatively, aFGF might modulate cellular responses less directly

by either inducing or repressing expression of other mediators.

Since aFGF can induce expression of plasminogen activators in fibroblasts (30) and endothelial cells (M. Presta, D. Mullins, D. Moscatelli, K.A.T., and D. Rifkin, unpublished observations) and repress expression of plasminogen activator inhibitor type 1 in endothelial cells (31) *in vitro*, it might also prevent local clot development and release of growth factors by degranulation of trapped platelets *in vivo*. Although no evidence for aFGF-mediated inhibition of clot development was observed 2 weeks after injury in this model, we cannot eliminate the possibility that clots had formed and dissolved.

In culture, vascular smooth muscle cells have been reported to transcribe and respond mitogenically to aFGF (32). Furthermore, aFGF induces cultured endothelial cell synthesis of platelet-derived growth factor A chain, a potent smooth muscle cell mitogen (33). Paradoxically, aFGF in the dose ranges studied here is found to inhibit intimal thickening, the end result of smooth muscle cell migration and proliferation and of extracellular matrix deposition. Although at the two highest infusion rates tested aFGF inhibits intimal proliferation, the magnitude is half that seen at the optimally efficacious dose rate. The diminished efficacy, however, is not necessarily the result of direct stimulation of smooth muscle cell proliferation. Endothelial cells *in vivo* might respond suboptimally to high concentrations of aFGF, a result observed with BALB/c 3T3 fibroblasts in culture (20). Additional studies will be required to characterize the effect of these dose levels of pure aFGF on smooth muscle cell migration, mitosis, and matrix deposition at sites of intravascular injury *in vivo*.

Much greater doses of the homologous basic FGF have been observed to enhance DNA synthesis not only of the leading edge of endothelial cells growing back over injured rat carotid arterial surfaces (34) but also of intimal smooth muscle cells (35). A 2-fold increase in intimal thickening occurs in response to 2 weeks of daily 12-μg i.v. injections for an estimated minimum total dose of $\approx$350 μg/kg. In contrast, inhibition of intimal thickening was achieved in this study with either a total aFGF dose of 0.29 μg/kg delivered by continuous i.v. infusion for 2 weeks or a single i.v. injection of aFGF (4.8 μg/kg) corresponding to $\approx$0.1% and $\approx$1%, respectively, of the basic FGF dose levels reported to enhance intimal thickening. At these elevated basic FGF dose levels, smooth muscle cells might be stimulated either directly or secondarily as a result of the modulation of other endocrine and paracrine systems.

Regardless of the mechanism, aFGF-mediated inhibition of intimal thickening at sites of intravascular damage could be therapeutically useful in humans. Similar intimal thickening following balloon angioplasty is the principal cause of coronary artery restenosis. Approximately 30% of human angioplasty sites undergo restenosis within 3–6 months (36). A significant decrease in this rate could improve the prognosis of patients receiving this increasingly widespread procedure.

This research was supported, in part, by a grant-in-aid from the Southeastern Pennsylvania Section of the American Heart Association (T.D.B. and M.D.) and by a Pharmaceutical Manufacturers Association Foundation Development Award for Clinical Pharmacology Units (T.D.B.).

1. Ross, R. (1986) *N. Engl. J. Med.* **314,** 488–500.
2. Munro, J. M. & Cotran, R. S. (1988) *Lab. Invest.* **58,** 249–261.
3. Clowes, A. W. & Schwartz, S. M. (1985) *Circ. Res.* **56,** 139–145.
4. Fishman, J. A., Rayan, G. B. & Karnovsky, M. J. (1975) *Lab. Invest.* **32,** 339–351.
5. Schwartz, S. M., Haudenschild, C. C. & Eddy, E. M. (1978) *Lab. Invest.* **38,** 568–580.
6. Clowes, A. W., Reidy, M. A. & Clowes, M. M. (1983) *Lab. Invest.* **49,** 208–215.
7. Reidy, M. A., Clowes, A. W. & Schwartz, S. M. (1983) *Lab. Invest.* **49,** 569–575.
8. Ishikawa, F., Miyazono, K., Hellman, U., Drexler, H., Wernstedt, C., Hagiwara, K., Usuki, K., Takaku, F., Risau, W. & Heldin, C.-H. (1989) *Nature (London)* **338,** 557–562.
9. Leung, D. W., Cachianes, G., Kuang, W.-J., Goeddel, D. V. & Ferrara, N. (1989) *Science* **246,** 1306–1309.
10. Keck, P. J., Hauser, S. D., Krivi, G., Sanzo, K., Warren, T., Feder, J. & Connolly, D. T. (1989) *Science* **246,** 1309–1312.
11. Conn, G., Bayne, M. L., Soderman, D. D., Kwok, P. W., Sullivan, K. A., Palisi, T. M., Hope, D. A. & Thomas, K. A. (1990) *Proc. Natl. Acad. Sci. USA* **87,** 2628–2632.
12. Klagsbrun, M. (1989) *Prog. Growth Factor Res.* **1,** 207–235.
13. Burgess, W. H. & Maciag, T. (1989) *Annu. Rev. Biochem.* **58,** 575–606.
14. Finch, P. W., Rubin, J. S., Miki, T., Ron, D. & Aaronson, S. A. (1989) *Science* **245,** 752–755.
15. Thomas, K. A., Rios-Candelore, M., Gimenez-Gallego, G., DiSalvo, J., Bennett, C., Rodkey, J. & Fitzpatrick, S. (1985) *Proc. Natl. Acad. Sci. USA* **82,** 6409–6413.
16. Terranova, V. P., DiFlorio, R., Lyall, R. M., Hic, S., Friesel, R. & Maciag, T. (1985) *J. Cell Biol.* **101,** 2330–2334.
17. Lobb, R. R., Alderman, E. M. & Fett, J. W. (1985) *Biochemistry* **24,** 4969–4973.
18. Herbert, J. M., Laplace, M. C. & Maffrand, J. P. (1988) *Int. J. Tissue Reac.* **3,** 133–139.
19. Dryjski, M., Mikat, E. & Bjornsson, T. D. (1988) *J. Vasc. Surg.* **8,** 623–633.
20. Linemeyer, D. L., Kelly, L. J., Menke, J. G., Gimenez-Gallego, G., DiSalvo, J. & Thomas, K. A. (1987) *Bio/Technology* **5,** 960–965.
21. Ortega, S., Schaeffer, M.-T., Soderman, D., DiSalvo, J., Linemeyer, D. L., Gimenez-Gallego, G. & Thomas, K. A. (1991) *J. Biol. Chem.* **266,** 5842–5846.
22. Clowes, A. W., Collazzo, R. E. & Karnovsky, M. J. (1978) *Lab. Invest.* **39,** 141–150.
23. Guyton, J. R., Rosenberg, R. D., Clowes, A. W. & Karnovsky, M. J. (1980) *Circ. Res.* **46,** 625–634.
24. Tallarida, R. & Murray, R. B. (1987) *Manual of Pharmacological Calculations with Computer Programs* (Springer, New York).
25. Alroy, J., Goyal, V. & Skutelsky, E. (1987) *Histochemistry* **86,** 603–607.
26. Bird, A. & Ling, N. (1987) *Biochem. Biophys. Res. Commun.* **142,** 428–435.
27. Rosengart, T. K., Kupferschmid, J., Ferrans, V. J., Casscells, W., Maciag, T. & Clark, R. E. (1988) *J. Vasc. Surg.* **7,** 311–317.
28. Greber, T. F., Kari, P. H., Hichens, M., Thomas, K. A., DiSalvo, J. & Vyas, K. P. (1990) *FASEB J.* **4,** A461 (abstr.).
29. Thompson, R. W. & D'Amore, P. A. (1987) *J. Mol. Cell. Cardiol.* **19,** S12 (abstr.).
30. Rappaport, R. S., Ronchetti-Blume, M., Vogel, R. L. & Hung, P. P. (1988) *Thromb. Haemostasis* **59,** 514–522.
31. Konkle, B. A. & Ginsburg, D. (1988) *J. Clin. Invest.* **82,** 579–585.
32. Winkles, J. A., Friesel, R., Burgess, W. H., Howk, R., Mehlman, T., Weinstein, R. & Maciag, T. (1987) *Proc. Natl. Acad. Sci. USA* **84,** 7124–7128.
33. Gay, C. G. & Winkles, J. A. (1990) *J. Biol. Chem.* **265,** 3284–3292.
34. Lindner, V., Majack, R. A. & Reidy, M. A. (1990) *J. Clin. Res.* **85,** 2004–2008.
35. Lindner, V., Lappi, D. A., Baird, A., Majack, R. A. & Reidy, M. A. (1991) *Circ. Res.* **68,** 106–113.
36. McBride, W., Lange, R. A. & Hillis, L. D. (1988) *N. Engl. J. Med.* **318,** 1734–1737.